


## ORIGINAL ARTICLE

# Nasopharyngeal cancer cell-derived exosomal PD-L1 inhibits CD8<sup>+</sup> T-cell activity and promotes immune escape

Jie Yang<sup>1</sup> | Jierong Chen<sup>2</sup> | Hu Liang<sup>3</sup> | Yahui Yu<sup>4</sup> 

<sup>1</sup>Department of Pathology, Zhujiang Hospital, Southern Medical University, Guangzhou, China

<sup>2</sup>Department of Clinical Laboratory, Guangdong Provincial People's Hospital, Guangdong Academy of Medical Sciences, Guangzhou, China

<sup>3</sup>Department of Nasopharyngeal Carcinoma, Sun Yat-Sen University Cancer Center, Guangzhou, China

<sup>4</sup>Department of Radiation Oncology, Zhujiang Hospital, Southern Medical University, Guangzhou, China

## Correspondence

Yahui Yu, Department of Radiation Oncology, Zhujiang Hospital, Southern Medical University, No. 253, Gongye Middle Avenue, Haizhu District, Guangzhou 510280, Guangdong Province, China.  
Email: [fish104@126.com](mailto:fish104@126.com)

## Funding information

China Postdoctoral Science Foundation, Grant/Award Number: 2019M663293; National Natural Science Foundation of China, Grant/Award Number: 81902750 and 82002855

## Abstract

Programmed cell death ligand 1 (PD-L1) is an immune surface protein that binds to programmed cell death 1 (PD-1) and allows tumors to evade T-cell immunity. This study aims to define the role of PD-L1 shuttled by tumor cell-derived exosomes in the immune escape of nasopharyngeal carcinoma (NPC). PD-L1 expression was determined in the exosomes isolated from the plasma of NPC patients or from NPC cells. It was found that PD-L1 was highly expressed in the exosomes from the plasma of NPC patients and also in the exosomes from NPC cells. PD-L1/PD-1 binding was identified in the presence or absence of interferon-gamma (IFN- $\gamma$ ) or anti-PD-L1 antibody. PD-L1 expression was elevated following IFN- $\gamma$  treatment. Binding of PD-L1 to PD-1 was augmented by IFN- $\gamma$  and blocked by anti-PD-L1 antibody. Following this, CD8<sup>+</sup> T cells were sorted out from peripheral blood samples to assess the binding between exosomal PD-L1 and PD-1 on the CD8<sup>+</sup> T-cell surface, and to measure the percentage of Ki-67-positive T cells. The results indicated that exosomal PD-L1 bound to the PD-1 on CD8<sup>+</sup> T-cell surface, leading to a reduced percentage of Ki-67-positive CD8<sup>+</sup> T cells and downregulated production of cytokines. In vivo data confirmed that exosomal PD-L1 promoted NPC tumor growth in mice by suppressing CD8<sup>+</sup> T-cell activity. In conclusion, NPC cell-derived exosomes deliver PD-L1 to bind to PD-1 on the CD8<sup>+</sup> T-cell surface, through which cytotoxic CD8<sup>+</sup> T-cell function was attenuated and the immune escape was thus promoted in NPC.

## KEYWORDS

CD8<sup>+</sup> T cells, exosomes, IFN- $\gamma$ , immune escape, nasopharyngeal carcinoma, programmed cell death ligand 1, programmed cell death-1

## 1 | INTRODUCTION

Nasopharyngeal carcinoma (NPC) is a malignant head and neck cancer type commonly occurring in specific geographical locations

including Southeast Asia and southern provinces of China.<sup>1,2</sup> Due to the intrinsic invasiveness as well as the asymptomatic nature of NPC, more than 60% of NPC patients are diagnosed at advanced stages, and the clinical outcomes for patients with recurrent/metastatic

**Abbreviations:** CPIs, checkpoint inhibitors; IFN- $\gamma$ , interferon-gamma; NC, negative control; NPC, nasopharyngeal carcinoma; NTA, nanoparticle tracking analysis; PD-1, programmed cell death 1; PD-L1, programmed cell death ligand 1; PMBCs, peripheral mononuclear blood cells; shRNA, short hairpin RNA; TILs, tumor-infiltrating lymphocytes.

Jie Yang, Jierong Chen and Hu Liang as co-first authors.

This is an open access article under the terms of the [Creative Commons Attribution-NonCommercial-NoDerivs](https://creativecommons.org/licenses/by-nc-nd/4.0/) License, which permits use and distribution in any medium, provided the original work is properly cited, the use is non-commercial and no modifications or adaptations are made.

© 2022 The Authors. *Cancer Science* published by John Wiley & Sons Australia, Ltd on behalf of Japanese Cancer Association.

NPC tumor are alarmingly poor in response to the radiotherapy and chemotherapy.<sup>3,4</sup> Herein, the development of novel therapies is imperative for NPC treatment.

Immune checkpoint inhibitors (CPIs) targeting the program cell death 1 (PD-1), or its ligand programmed cell death ligand 1 (PD-L1), have been indicated by accumulating evidence to exhibit durable clinical responses across cancer types.<sup>5,6</sup> The PD-1 receptor on tumor cells has been established as a critical negative modulator, when engaged by its ligand PD-L1, of T-cell-mediated cellular immune responses.<sup>7,8</sup> Inflammation-induced PD-L1 expression in the tumor microenvironment induces PD-1-mediated T-cell exhaustion, attenuating the antitumor effects of cytotoxic T cells.<sup>9</sup>

Of note, PD-L1 is highly expressed in NPC, responsible for the poor prognosis,<sup>10</sup> indicating the great potential of PD-1/PD-L1 blockade immunotherapy in the treatment of NPC. Furthermore, up-regulated expression of PD-L1 has been detected in plasma-derived exosomes from various cancers, and tumor-derived exosomes could shuttle PD-L1 intercellularly to confer resistance to immune checkpoint therapy.<sup>11</sup> Nonetheless, the role of exosomal PD-L1 in the pathogenesis of NPC remains unclear. Moreover, accumulating evidence has elucidated that PD-L1 on the surface of tumor cells may be upregulated by interferon-gamma (IFN- $\gamma$ ) secreted by activated CD8+ T cells, and that PD-L1 binding to PD-1 can promote the immune escape in cancers through inhibiting T-cell functions.<sup>12,13</sup>

This study aims to delineate a hypothesized mechanism by which PD-L1 delivered by exosomes binds to PD-1, inactivates cytotoxic CD8+ T cells, and thereby promotes the immune escape in NPC.

## 2 | MATERIALS AND METHODS

### 2.1 | In silico prediction

NPC-related gene expression datasets GSE53819 and GSE61218 were obtained from the GEO database. The GSE53819 dataset includes 16 normal samples and 16 NPC samples while the GSE61218 dataset includes six normal samples and 10 NPC samples. Differential analysis was performed using the GEO2R tool to screen the significantly highly-expressed genes with  $\log_{2}FC > 1.7$  and  $P < 0.01$  as the threshold. The top 100 genes associated with NPC were retrieved from GeneCards with "nasopharyngeal carcinoma" as the key word.

R language was used to draw a box plot of the expression of key genes, and 10 interacting genes of key genes were predicted using the STRING database. The MEM database was applied for co-expression analysis. The KOBAS database was used to perform GO and KEGG enrichment analysis of the key genes and 10 interacting genes to determine the function of key genes.

### 2.2 | Patient enrollment

Plasma samples were collected from 25 patients with NPC at Sun Yat-Sen University Cancer Center (SYSUCC) from 2017 to 2020, and the

collected samples were pathologically validated to be NPC. None of the participants had been treated by chemotherapy or radiotherapy before biopsy or plasma collection. Meanwhile, 25 healthy donors were recruited to harvest the normal plasma samples as a healthy control. The current study was performed in line with the Declaration of Helsinki and approved by the Clinical Ethics Committee of SYSUCC. All participants signed written informed consent.

### 2.3 | Cell culture

Four NPC cell lines (C666-1, HK-1, HNE3, NPC-TW01), human normal nasopharyngeal cell line NP69, and human embryonic kidney cell line HEK-293T were acquired from the Institute of Biochemistry and Cell Biology, Shanghai Institutes for Biological Sciences, Chinese Academy of Sciences. HK-1, C666-1, HNE3, and NP69 cells were cultured with RPMI 1640 medium (Gibco) with 10% fetal bovine serum (FBS; Gibco), 100  $\mu\text{g}/\text{ml}$  streptomycin (Gibco), and 100 U/ml penicillin (Gibco). NPC-TW01 and HEK-293T cells were cultured with DMEM (Gibco) with 10% FBS, 100  $\mu\text{g}/\text{ml}$  streptomycin, and 100 U/ml penicillin. These cells were cultured in an incubator at 37°C with 5% CO<sub>2</sub>. C666-1 cells were treated with 100 ng/ml recombinant human IFN- $\gamma$  (C600039-0020, Sangon Biotech) for 48 h, and the stimulating effect of IFN- $\gamma$  on PD-L1 was detected.

### 2.4 | Lentivirus-mediated transduction

C666-1 cells were grouped and transduced with lentivirus carrying short hairpin RNA (shRNA) targeting PD-L1 or corresponding negative control (NC), referred as the sh-PD-L1 or the sh-NC group. All lentivirus purchased from Genechem was labeled with GFP. Before the formal assay, C666-1 cells incubated in 96-well plates were transduced with lentivirus that had been diluted with PBS into different titers, and 24 h later the GFP intensity was detected by a fluorescence microscopy to identify the titer with the strongest fluorescence intensity. For the formal transduction, the cells were incubated in 24-well plates (5  $\times 10^4$  cells/well) and were added with lentivirus (in the previously selected titer) along with 10  $\mu\text{g}/\text{ml}$  Polybrene (H8761, Solarbio) when they reached the logarithmic growth phase; the medium was renewed after 16–24 h, and 1  $\mu\text{g}/\text{ml}$  puromycin (A1113803, Invitrogen) was added 72 h later for the sorting of stably transduced cells.

### 2.5 | qRT-PCR and Western blot assay

Total RNA was extracted from the cells utilizing TRIzol reagent. RNA quantification was performed with the Fast SYBR Green PCR kit and the ABI PRISM 7300 RT-PCR system. The  $2^{-\Delta\Delta\text{Ct}}$  method was adopted to calculate transcription levels of the target gene, normalized to GAPDH (Table S1).

Cells were lysed with RIPA lysis buffer with 1% protease inhibitor and 1% phosphatase inhibitor. Exosomal protein was extracted

from the plasma utilizing the Exosome Isolation Kit. Protein lysate was separated with 10% SDS-PAGE and transferred to a PVDF membrane, which was blocked with 5% BSA. Subsequently, the protein-loading membrane was incubated with primary antibodies (Table S2) and with HRP-labeled secondary antibodies. Immunoreactive bands were visualized using ECL. Quantitative protein analysis was then conducted with ImageJ 1.48u software. Relative protein expression was expressed as the ratio of the gray values of the target protein to those of the internal reference GAPDH.

## 2.6 | Isolation of exosomes from cells and plasma

Exosomes in cells were isolated by ultracentrifugation: the cells were cultured in RPMI 1640 medium with 10% exosome-free FBS for 48 h and subjected to 20 min of centrifugation ( $2 \times 10^3 g$ ) at 4°C and another 30 min of centrifugation ( $1 \times 10^4 g$ ) to remove cell debris. The obtained supernatant was filtered through a 0.2- $\mu m$  filter (Micropore) and then ultracentrifuged ( $1 \times 10^5 g$ ) for 1 h. The precipitate was resuspended in PBS and subjected to 1 h of ultracentrifugation ( $1 \times 10^5 g$ ) at 4°C, followed by extraction of exosomes from the supernatant utilizing EXO Rapid Precipitation Solution (SBI). The size and distribution of exosomes were then detected with nanoparticle tracking analysis (NTA) utilizing a NanoSight NS300 system (Malvern Instruments).

Exosomes in the plasma were isolated by differential centrifugation: anticoagulated venous blood samples of patients or healthy donors were centrifuged (1550g, 30 min) to obtain cell-free plasma (Allegra X-14R, Beckman Coulter), which was then centrifuged at 16,500g for 45 min (5418R, Eppendorf). The precipitated cell microbubbles were resuspended with PBS and subjected to 2 h of centrifugation (100,000g, 4°C) to precipitate exosomes (Optima™ MAX-XP, Beckman Coulter).

## 2.7 | TEM

The extracted exosomes were characterized using a TEM. Briefly,  $1 \times 10^8$  exosomes were resuspended and fixed with 30  $\mu l$  of 2% paraformaldehyde and then transferred to the discharged copper grid. Next, the exosome-loading copper grid was immersed in 3% glutaraldehyde for fixation, followed by staining of exosomes using 4% uranyl acetate (added dropwise). Images of the exosomes were photographed under a TEM (FEI Apreo, Thermo Fisher Scientific).

## 2.8 | Flow cytometric sorting of CD8+ T cells

Peripheral mononuclear blood cells (PMBCs) were isolated from the peripheral blood of healthy volunteers utilizing Ficoll density gradient centrifugation. The single cell suspension was then incubated for 45 min with CD8 fluorescent antibody (#55397, CST) at 4°C in the dark and diluted with serum-free medium, followed by sorting of CD8+ T cells with a flow cytometry system (MoFloAstrios EQ, Beckman Coulter).

## 2.9 | Detection of the binding of exosomal PD-L1 to PD-1

Initially, 100- $\mu l$  processed Exo samples at different concentrations were added to a 96-well ELISA plate that had been coated with PD-L1 antibody (#13684, CST) for overnight incubation at 4°C. The next day samples were probed with 100  $\mu l$  biotin-labeled human PD-1 protein (4  $\mu g/ml$ ; 71,109, BPS Bioscience) for another 2 h, and with 100  $\mu l$  HRP-conjugated streptavidin (BD Biosciences) with 0.1% BSA for 1 h. After that, tetramethylbenzidine (Pierce) was added dropwise to the plate for the detection of the OD, with 0.5 N  $H_2SO_4$  added to terminate the development. Next, a BioTek microplate reader was utilized to determine the OD of the plate at a wavelength of 450 nm.

## 2.10 | ELISA

PD-L1 concentration on exosomes was analyzed by serial dilution, and the concentration of PD-L1 in exosomes derived from cells or plasma was calculated based on ELISA analysis. The CD8+ T-cell supernatant was collected to detect the contents of IFN- $\gamma$  (#BMS228), TNF- $\alpha$  (#KHC3011), and interleukin (IL)-2 (#EH2IL2) following the protocols of corresponding kits (Thermo Fisher Scientific).

## 2.11 | CD8+ T-cell proliferation

To block the PD-L1 from the surface of exosomes, purified exosomes (200  $\mu g$ ) along with the PD-L1 antibody (10  $\mu g/ml$ ) or IgG isotype antibody (10  $\mu g/ml$ ) were incubated in 100  $\mu l$  PBS, followed by ultracentrifugation to remove unbound, free antibodies. CD8+ T cells were stimulated using 2  $\mu g/ml$  anti-CD3 (#86603, CST) and 2  $\mu g/ml$  anti-CD28 (#38774, CST) antibodies for 24 h, and then subjected to 2 h of incubation with cell-released exosomes (with/without the blocking of PD-L1) in response to anti-CD3/CD28 antibodies. Subsequently, CD8+ T cells were labeled with CFSE, a dye (molecular probe) that tracks cell division, through a 20-min co-incubation (5  $\mu M$  CFSE was applied for labeling of  $1 \times 10^6$  CD8+ T cells) at 37°C, which was terminated by the addition of cold medium (five times the volume of the co-cultured mixture) supplemented with 10% FBS; CD8+ T cells without co-culture with exosomes were set as the control group.

## 2.12 | Identification of the binding of exosomes to CD8+ T cells

The aforementioned CFSE-labeled exosomes were precipitated by ultracentrifugation. CD8+ T cells were labeled with Alexa Fluor 647 fluorescent Anti-CD8 alpha antibody (ab237365, 1:100, Abcam). Subsequently, the exosomes (25  $\mu g/ml$ ) were then incubated for 2 h with CD8+ T cells that had been treated by anti-CD3/CD28 antibodies or not ( $2 \times 10^5$  cells/well in a 96-well plate), followed by flow cytometry or a confocal microscopy to detect the binding of exosomes to the surface of CD8+ T cells.

## 2.13 | Immunofluorescence staining

Sections were subjected to antigen retrieval, blocked with 5% BSA, and then incubated at 4°C overnight with primary antibody against CD8 (1:400, #55397, CST) prepared from goat serum. Afterwards, sections were probed with the secondary antibody (fluorescent goat anti-mouse IgG, #4417, CST), followed by another incubation with DAPI. Observation and photography were performed utilizing an Olympus confocal microscope (FV1200).

## 2.14 | Establishment of a xenograft mouse model

A total of 30 male CD34+ HSC-transferred humanized mice (6–8 weeks, 18–22 g; Phenotek Co., Ltd) were housed (five mice per cage) for 1 week before the experiment for acclimatization in a ventilated animal room (22°C, under a 12-h light/dark cycle), with free access to water and food.

The mice were subcutaneously injected with C666-1 cells stably knocking down PD-L1 or the NC cells (i.e. sh-PD-L1-treated or sh-NC-treated cells,  $5 \times 10^6$  cells in 100  $\mu$ l PBS) into the flank region.

Specifically, the mice were classified into five groups ( $n = 6$ ) according to the different injections: sh-PD-L1+saline (injection of sh-PD-L1-treated C666-1 cells+saline), sh-PD-L1+EXO (injection of sh-PD-L1-treated C666-1 cells and C666-1 cell-derived exosomes), sh-PD-L1+EXO+IgG (injection of sh-PD-L1-treated C666-1 cells, C666-1 cell-derived exosomes and NC IgG antibody), sh-PD-L1+EXO+PD-L1-Ab (injection of sh-PD-L1-treated C666-1 cells, C666-1 cell-derived exosomes and PD-L1 monoclonal antibody [Atezolizumab, Roche; 100  $\mu$ g per injection, three times a week for 2 weeks]), sh-NC+saline (injection of sh-NC-treated C666-1 cells and saline), and sh-NC+GW4869 (injection of sh-NC-treated C666-1 cells and the exosome secretion inhibitor GW4869) groups.

Of note, C666-1 cell-derived exosomes were injected via tail vein every 3 days (100  $\mu$ g each time, dissolved in 100  $\mu$ l PBS). During the treatment period, the diameter of the tumor was detected every 5 days and the tumor volume was calculated: longest diameter  $\times$  shortest diameter<sup>2</sup>  $\times$  0.5. When the longest diameter of the tumor reached 20 mm, the mice were euthanized. Animal experiments were performed following *Guide for the Care and Use of Laboratory Animals* published by the National Institutes of Health, and approved by the Animal Ethics Committee of SYSUCC.

## 2.15 | Statistical analysis

SPSS 21.0 software was adopted for statistical analysis. Measurement data were displayed as mean  $\pm$  SD. The difference was statistically significant at  $P < 0.05$ . An independent-sample *t* test was used for two-group data comparison, one-way ANOVA with Tukey's test for multi-group data comparison, and Tukey-corrected repeated measures ANOVA for multi-group data comparison at different time points.

## 3 | RESULTS

### 3.1 | PD-L1 is highly expressed in exosomes derived from the plasma of NPC patients

We performed differential analysis of the NPC-related GSE53819 and GSE61218 microarrays to explore the mechanisms underlying the occurrence and development of NPC. As a result, 283 and 494 overexpressed genes in NPC samples were identified, respectively, and the top 100 NPC-associated genes were predicted through the GeneCards database. The differential analysis results of GSE53819 and GSE61218 microarrays were then intersected with the prediction results of the GeneCards database, which included four genes: PD-L1 (NCBI: CD274), MMP1, PTGS2, and KRT5 (Figure 1A).

Further, box plots of PD-L1 expression were constructed based on the microarray analysis, which confirmed the overexpression of PD-L1 occurring in NPC tissue samples versus normal tissue samples (Figure 1B,C). Prior evidence has indicated that PD-L1 was enriched in plasma-derived exosomes.<sup>14</sup> Herein, we separated exosomes from the plasma samples of 25 NPC patients and from plasma samples of healthy donors (referred to as the Normal group) by ultracentrifugation. Subsequent ELISA results showed amplified PD-L1 in exosomes as well as in the peripheral blood from NPC patients, as compared with those from the Normal group, while no obvious difference was found in peripheral blood PD-L1 between the two groups when exosomes had been removed from the blood (Figure 1D).

These results suggest that PD-L1 is highly expressed in exosomes from the plasma of NPC patients.

### 3.2 | PD-L1 overexpression occurs in NPC cell-derived exosomes

Next, we observed PD-L1 expression in NPC cell-derived exosomes. We isolated exosomes from four NPC cell lines (C666-1, HK-1, HNE3, and NPC-TW01) and a human normal nasopharyngeal NP69 cell line, observed the separated exosomes by TEM, and examined the size and distribution using the NanoSight system. According to the results, the exosomes were all double-membrane vesicles with diameters of 50–150 nm (Figure 2A,B). Western blot assay results revealed high expression of CD63, CD9, TSG101, and Alix in the extracted exosomes, while Calnexin expression was absent (Figures 2C and S1), indicating the successful separation of exosomes. The expression of PD-L1 was upregulated in NPC cell-derived exosomes relative to that in cell extracts, and higher in NPC cell-derived exosomes as compared with that in NP69 cell-derived exosomes. Among the four NPC cell lines, C666-1 cell-derived exosomes presented with the highest PD-L1 expression and were thus applied in subsequent assays (Figures 2C and S1). Collectively, these results indicate the upregulation of PD-L1 in exosomes from NPC cells.

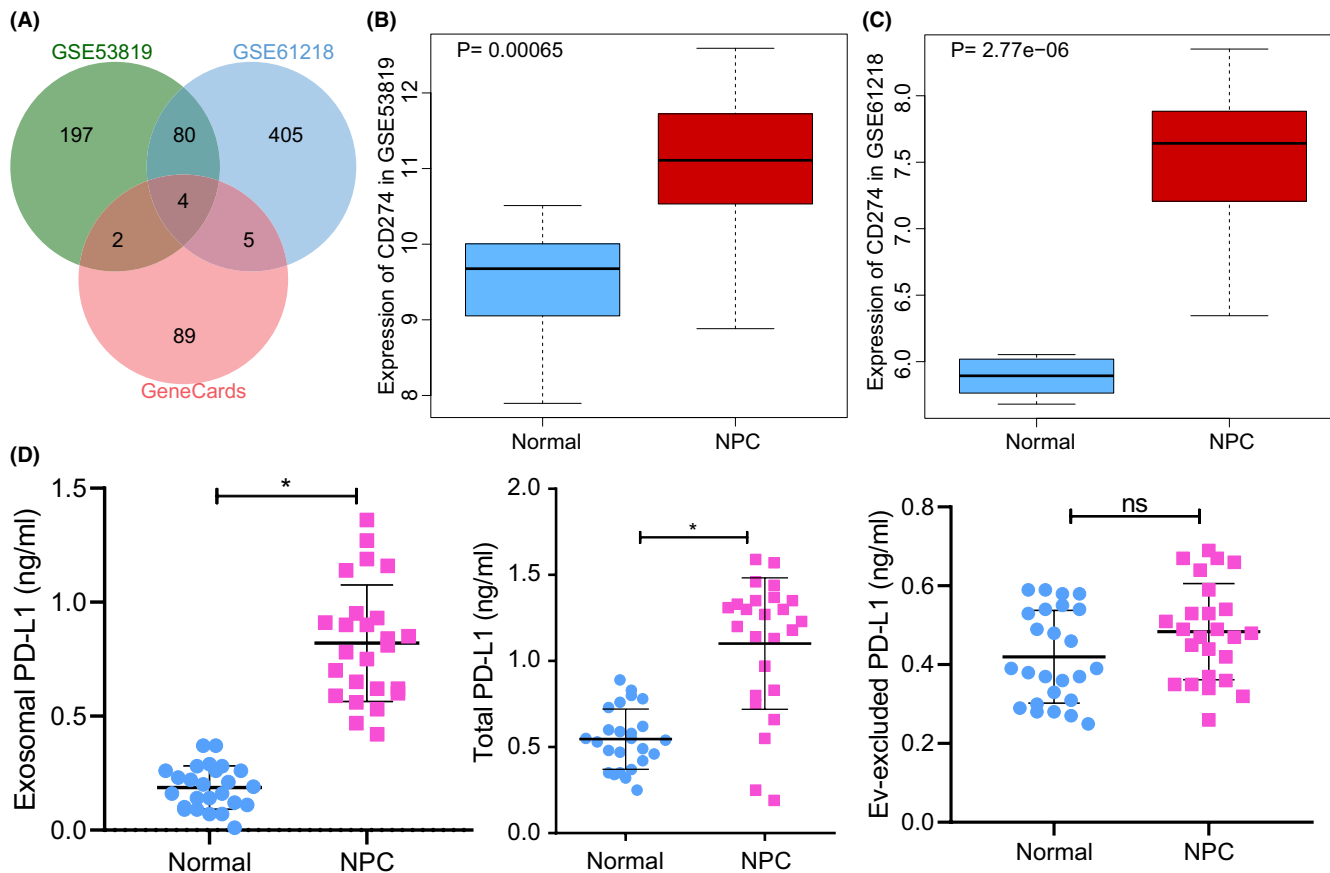


**FIGURE 1** PD-L1 was enriched in exosomes derived from the plasma of NPC patients. (A) Venn plot of the highly expressed genes from the GSE53819 and GSE61218 microarray datasets and the top 100 NPC-related genes predicted by the GeneCards database. (B) A box plot of the PD-L1 expression in normal samples (blue,  $n = 16$ ) and NPC samples (red,  $n = 16$ ) in the GSE53819 microarray. (C) A box plot of the PD-L1 expression in normal samples (blue,  $n = 6$ ) and NPC samples (red,  $n = 10$ ) in the GSE61218 microarray. (D) Content of PD-L1 in the exosomes derived from plasma samples, in peripheral blood, and in peripheral blood with exosomes removed, all from NPC patients (NPC group,  $n = 25$ ) and healthy donors (Normal group,  $n = 25$ ) detected by ELISA. \* $P < 0.05$ ; ns, not significant

### 3.3 | IFN- $\gamma$ promotes PD-L1 binding to PD-1 and the binding can be abolished by anti-PD-L1 antibody

Following the aforementioned finding, we then explored the potential correlation between the upregulated expression of PD-L1 in NPC-derived exosomes and the progression of NPC. By prediction using the STRING database, PD-1 (NCBI name: PDCD1) was identified to be the gene with the highest score for interaction with PD-L1 (Figure 3A). MEM analysis then verified the significant co-expression of PD-L1 and PD-1 (Figure 3B). Furthermore, KOBAS-based GO and KEGG enrichment analyses displayed that the genes interacting with PD-L1 were mainly related to T-cell activities (Figure 3C). Since the PD-L1 binding to PD-1 has been demonstrated to promote the immune escape in cancers through inhibiting T-cell functions,<sup>13</sup> we speculated that the NPC plasma or cell-derived exosomes transferred PD-L1 to bind to PD-1 to mediate the immune escape of NPC, thus contributing to the development of NPC.

To examine the speculation, we conducted ELISA and Western blot assay, wherein the expression of PD-L1 in the exosomes

derived from C666-1 cells was upregulated in response to IFN- $\gamma$  (Figure 3D,E). The C666-1 cells were treated with IFN- $\gamma$  and anti-PD-L1 antibody, and different concentrations of exosomes were extracted. ELISA results confirmed that exosomal PD-L1 bound to PD-1 in a concentration-dependent manner, and that the binding could be augmented by IFN- $\gamma$  but inhibited by the anti-PD-L1 antibody (Figure 3F).

These results suggest that PD-L1 expression is elevated by IFN- $\gamma$  and the binding of PD-L1 to PD-1 is blocked by the anti-PD-L1 antibody.

### 3.4 | Exosomal PD-L1 binds to PD-1 on CD8+ T-cell surface to promote the immune escape in NPC

Notably, the current model for PD-L1-modulated immune escape is attributed to the interaction between PD-L1 on the tumor cell surface and PD-1 on the CD8 T cells.<sup>15</sup> Herein, we then managed to investigate whether exosomal PD-L1 inhibited CD8+ T cells. We sorted out CD8+ T cells from peripheral blood mononuclear cells using flow

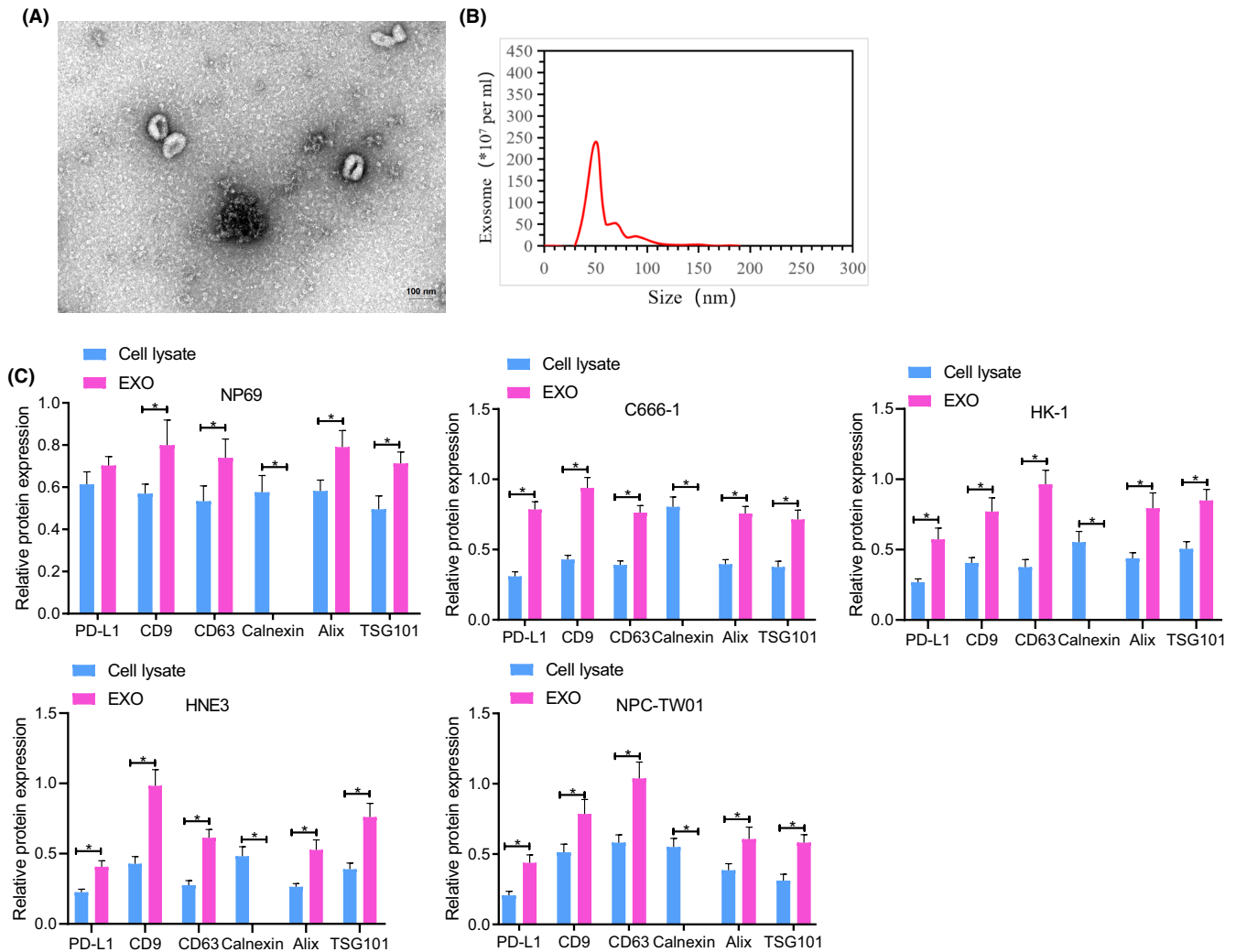


**FIGURE 2** PD-L1 was enriched in exosomes derived from NPC cells. (A) TEM observation of the morphology of the exosomes isolated from NPC cells (represented by C666-1 cell-derived exosomes). (B) The size and distribution of NPC cell-derived exosomes (represented by C666-1 cell-derived exosomes) measured by NTA. (C) Western blot assay of the protein expression of PD-L1, CD63, CD9, Calnexin, TSG101, and Alix in exosomes (labeled as EXO) from four NPC cell lines and in cell extracts (labeled as Cell lysate). Each cellular experiment was repeated three times. \* $P < 0.05$

cytometry (Figure 4A), and co-cultured the CFSE-labeled C666-1 cell-derived exosomes with the CD8<sup>+</sup> T cells unstimulated or stimulated using anti-CD3/CD28 antibodies for 2 h. Subsequent confocal microscopic observation results showed that exosomal PD-L1 interacted with PD-1 on the CD8<sup>+</sup> T cell surface (Figure 4B). In addition, the interaction between stimulated CD8<sup>+</sup> T cells using anti-CD3/CD28 antibodies and exosomal PD-L1 was stronger than that of unstimulated CD8<sup>+</sup> T cells and exosomal PD-L1. Meanwhile, exosomes from IFN- $\gamma$ -treated C666-1 cells, versus those from untreated cells, presented with a more pronounced increase in the binding between exosomal PD-L1 and activated CD8<sup>+</sup> T cells (Figure 4C,D). Furthermore, the results of qRT-PCR showed that PD-1 expression on the surface of CD8<sup>+</sup> T cells stimulated with anti-CD3/CD28 antibodies was higher than that on the unstimulated CD8<sup>+</sup> T-cell surface. However, PD-1 expression was further increased on the surface of stimulated CD8<sup>+</sup> T cells following co-culture with the exosomes from IFN- $\gamma$ -treated C666-1 cells (Figure S2).

Next, we assessed the effect of PD-L1 interacting CD8<sup>+</sup> T cells on cellular immune function. According to results of flow cytometry, co-culture with the exosomes led to a reduced proportion of CD8<sup>+</sup> T cells as well as a reduced percentage of Ki-67-positive cells, and these reductions were reversed in response to the additional treatment by anti-PD-L1 antibody. No difference was observed in the proportion of CD8<sup>+</sup> T cells and the percentage of Ki-67-positive cells between the control CD8<sup>+</sup> T cells and the CD8<sup>+</sup> T cells treated with EXO + PD-L1-Ab (Figure 4E,F). ELISA results indicated that expression of IFN- $\gamma$ , IL-2, and TNF- $\alpha$  in CD8<sup>+</sup> T cells was decreased in response to the co-culture with exosomes, and the decrease was negated following anti-PD-L1 antibody. Additionally, there appeared no difference in the expression of IFN- $\gamma$ , IL-2, and TNF- $\alpha$  between the control CD8<sup>+</sup> T cells and the CD8<sup>+</sup> T cells treated with EXO + PD-L1-Ab (Figure 4G).

Collectively, our data demonstrated that NPC cell-derived exosomal PD-L1 bound to the PD-1 on CD8<sup>+</sup> T cell surface to promote

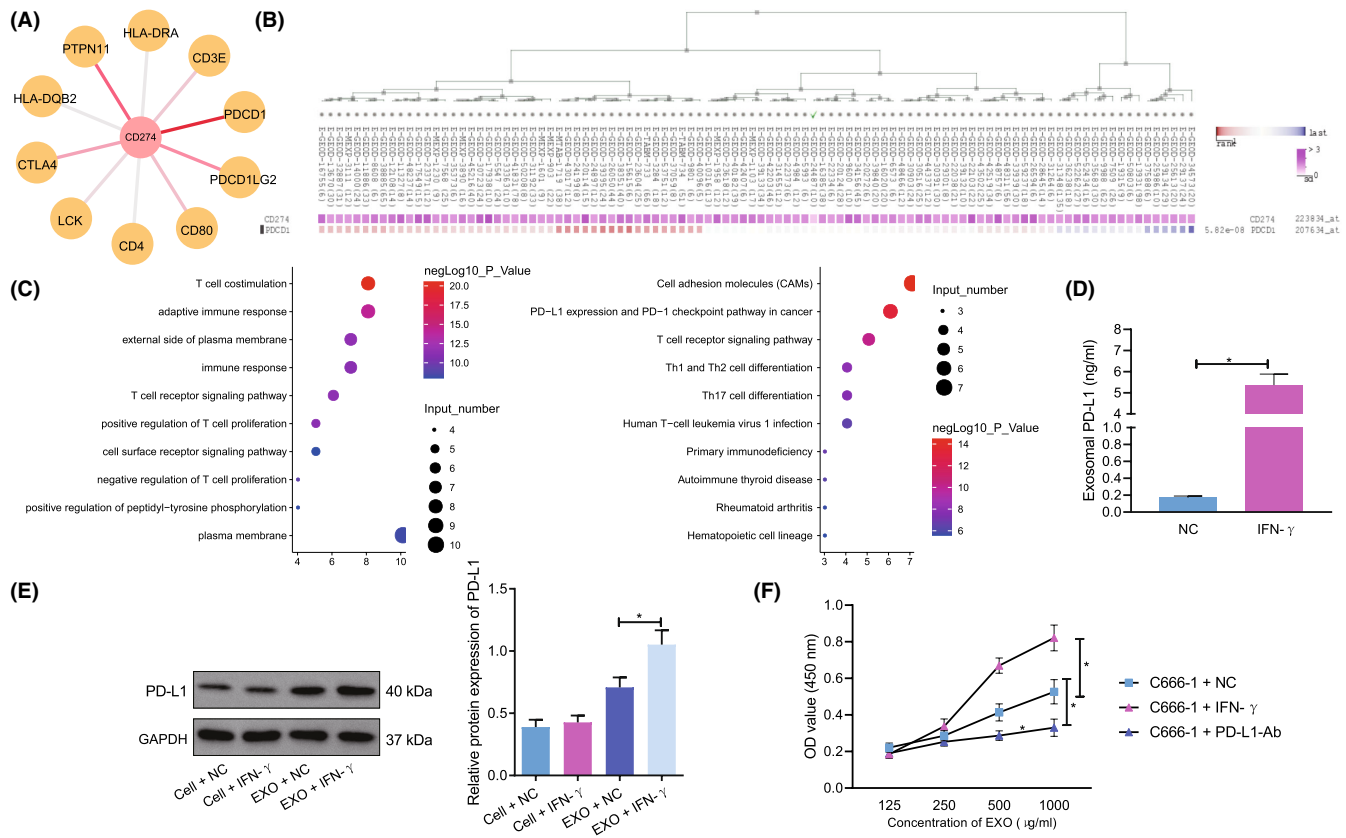


**FIGURE 3** PD-L1 bound to PD-1. (A) Prediction of 10 PD-L1 interacting genes based on the STRING database (the darker red lines between two genes indicate a higher score of interaction and PD-1 is the highest score). (B) An obvious co-expression between PD-L1 and PD-1, predicted by the MEM tool (<https://biit.cs.ut.ee/mem/index.cgi>). (C) The GO (left) and KEGG (right) pathway enrichment analyses of PD-L1 and its interacting genes, with the vertical axis representing the enriched items (the top 10) and the horizontal axis representing the number of genes enriched in the item. The color of the bubble, as shown by the color scale on the right, indicates the  $-\log_{10}P$  value regarding the item. (D) PD-L1 expression in exosomes derived from IFN- $\gamma$ -treated C666-1 cells measured by ELISA. (E) Western blot assay of PD-L1 expression in exosomes derived from IFN- $\gamma$ -treated C666-1 cells. (F) The binding between PD-L1 and PD-1 in exosomes derived from C666-1 cells treated with IFN- $\gamma$  or anti-PD-L1 antibody (the OD450 value indicates the binding affinity between the two) measured by ELISA. \* $P < 0.05$ . Each cellular experiment was repeated three times

exhaustion of activated CD8+ T cells, thereby driving the immune escape in NPC.

### 3.5 | Exosomal PD-L1 accelerates the tumorigenicity of NPC cells in vivo

Following the aforementioned in vitro findings, we then moved to in vivo substantiation. We knocked down PD-L1 in C666-1 cells by lentivirus-mediated sh-PD-L1 treatment, the silencing efficiency of which was validated by qRT-PCR. The expression of PD-L1 was reduced in C666-1 cells and C666-1 cell-derived exosomes on sh-PD-L1 (Figure 5A). In addition, the NTA results demonstrated no significant difference in the concentration and particle size of exosomes (Figure S3).

These sh-PD-L1-treated C666-1 cells or sh-NC-treated C666-1 cells were then injected into the mice subcutaneously, and C666-1 cell-derived exosomes or GW4869 (exosome secretion inhibitor) were injected through tail vein, with/without further treatment of the mice by PD-L1 monoclonal antibody. The volume of resected tumors of mice was measured every 5 days. According to the results,

the volume and weight of the tumors were reduced in response to treatment with sh-PD-L1 or GW4869. In addition, the co-culture of sh-PD-L1-treated C666-1 cells with exosomes, as compared with the cells alone, led to increased volume and weight of the tumors in mice, and these increases were abrogated following additional treatment by anti-PD-L1 antibody. Meanwhile, the injection of either sh-PD-L1-treated C666-1 cells or GW4869 was observed to reduce the weight and volume of mouse tumors, relative to the injection of NC cells and saline (Figure 5B-D).

Furthermore, we conducted immunofluorescence to detect the infiltration of CD8+ T tumor-infiltrating lymphocytes (TILs) in mouse tumor tissues. The results showed that the infiltration of CD8+ TILs was increased in response to treatment with sh-PD-L1 or GW4869. Additionally, the infiltration of CD8+ TILs was reduced in response to sh-PD-L1-treated C666-1 cells with exosomes but again enhanced by additional treatment by anti-PD-L1 antibody. In addition, the injection of either sh-PD-L1-treated C666-1 cells or GW4869 was observed to elevate the infiltration in CD8+ TILs (Figure 5E).

In summary, these results indicate that exosomal PD-L1 promoted the tumor growth of NPC cells in vivo by attenuating CD8+ T cell activity, which could be undermined by anti-PD-L1 antibody.

## 4 | DISCUSSION

It has been suggested that PD-L1-overexpressing tumor cells display exceptional capabilities to escape the immune system surveillance.<sup>16</sup> In the present study, we elucidated that PD-L1 loaded by NPC cell-derived exosomes contributed to the immune escape in NPC through inactivating CD8+ T cells via the PD-L1 binding to PD-1 on T cell surface.

Cancer cells generally produce more exosomes relative to normal cells, and numerous studies have confirmed the promoting effects of exosomes released by tumor cells on various cell malignant behaviors such as immune escape, tumor epithelial-mesenchymal transition, and angiogenesis.<sup>17,18</sup> In this study, our initial investigation showed abundant PD-L1 in exosomes derived from the plasma of NPC patients, and we then identified the upregulation of PD-L1 in exosomes from NPC cells. Our findings corroborate previous

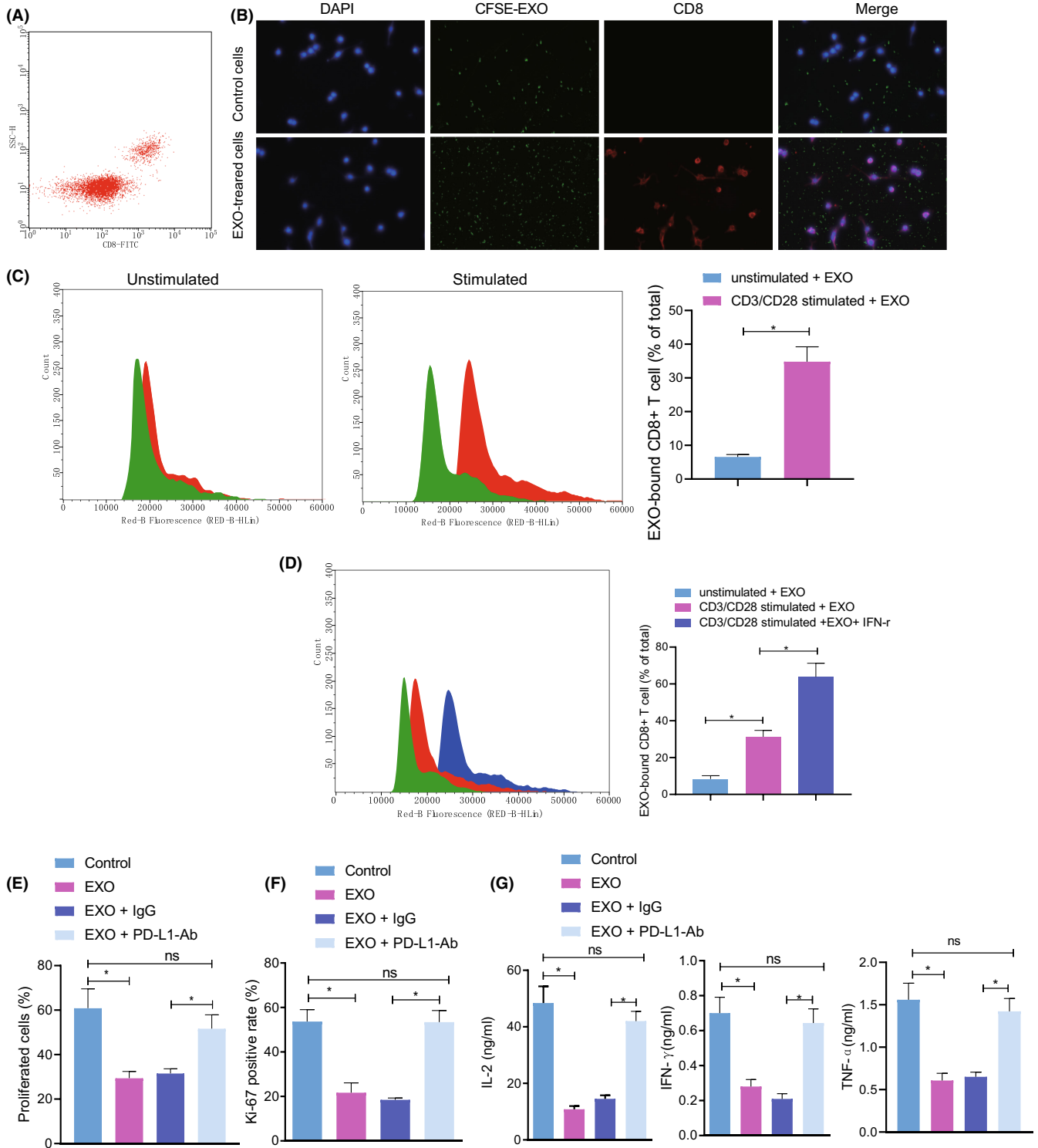




**FIGURE 4** The binding of PD-L1 to PD-1 promotes the immune escape in NPC cells. (A) Flow cytometric sorting of CD8<sup>+</sup> T cells from human peripheral blood mononuclear cells. (B) Confocal microscopic observation of CFSE-labeled C666-1 cell-derived exosomes binding to PD-1 on the CD8<sup>+</sup> T-cell surface. In this panel, unstimulated+EXO indicates that the CD8<sup>+</sup> T cells unstimulated with anti-CD3/CD28 antibodies were co-cultured with CFSE-labeled C666-1 cell-derived exosomes. CD3/CD28 stimulated+EXO indicates that the CD8<sup>+</sup> T cells stimulated with anti-CD3/CD28 antibodies were co-cultured with CFSE-labeled C666-1 cell-derived exosomes. CFSE-EXO indicates the CFSE-labeled exosomes. (C) Flow cytometric analysis of the binding ratio between C666-1 cell-derived exosomes and activated/inactivated CD8<sup>+</sup> T cells (i.e. CD8<sup>+</sup> T cells with/without pre-stimulation by anti-CD3/CD28 antibodies). The green curve in the figure represents the fluorescence intensity of CFSE in the control group, and the red curve represents the fluorescence intensity of CFSE after activation. (D) Flow cytometric analysis of the binding ratio between exosomes from IFN- $\gamma$ -treated C666-1 cell and activated CD8<sup>+</sup> T cells. The green curve in the figure represents the fluorescence intensity of CFSE in the unstimulated+EXO group, and the red and blue curves represent the fluorescence intensity of CFSE in the CD3/CD28 stimulated+EXO group and the CD3/CD28 stimulated+EXO+IFN- $\gamma$  group, respectively. (E) Flow cytometric analysis of the proportion of CD8<sup>+</sup> T cells in response to co-culture with the exosomes alone or in combination with treatment by anti-PD-L1 antibody. (F) Flow cytometric analysis of the proportion of Ki-67-positive cells in CD8<sup>+</sup> T cells in response to co-culture with the exosomes alone or in combination with treatment by anti-PD-L1 antibody. (G) Levels of IFN- $\gamma$ , IL-2, and TNF- $\alpha$  in CD8<sup>+</sup> T cells in response to co-culture with the exosomes alone or in combination with treatment by anti-PD-L1 antibody measured by ELISA. \* $P < 0.05$ . Each cellular experiment was repeated three times

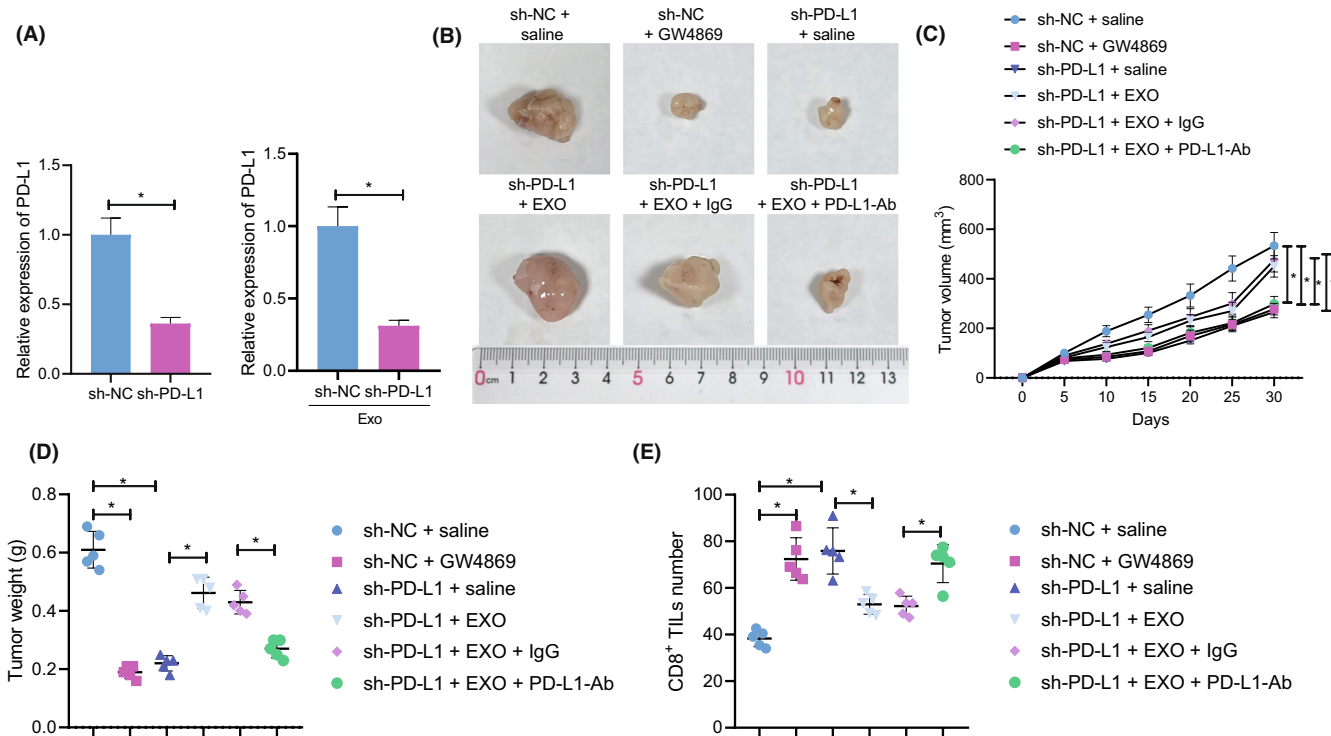


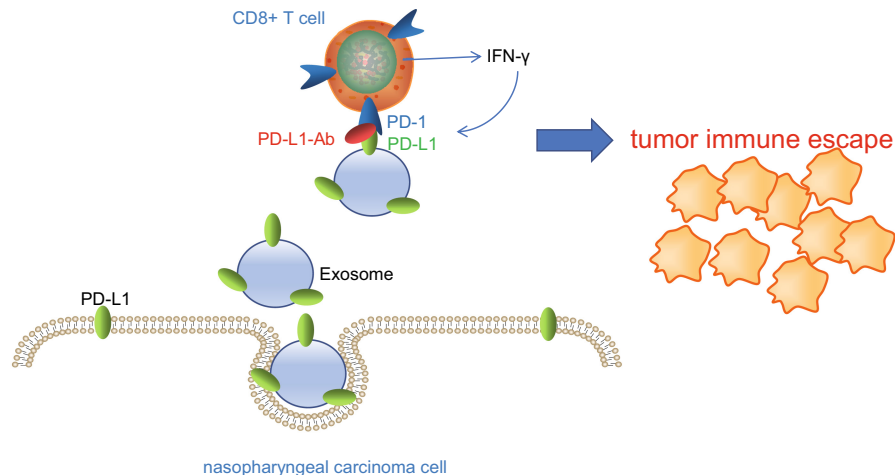
**FIGURE 5** Exosomal PD-L1 facilitates the tumor growth of NPC cells in mice. (A) The knockdown efficiency of lentivirus-mediated sh-PD-L1 treatment in C666-1 cells validated by qRT-PCR. (B) Images of NPC cell-implanted tumors in mice of each group. (C) The volume of NPC cell-implanted tumors in mice of each group, measured every 5 days. (D) The weight of NPC cell-implanted tumors in mice of each group. (E) Immunohistochemical staining of the infiltration of CD8<sup>+</sup> TILs in tumor tissues of mice of each group (the y axis represents the number of CD8<sup>+</sup> TILs in every five high-power fields of view). \* $P < 0.05$

reports on the co-overexpression of PD-L1 and PD-1 in NPC, associating with higher local recurrence and poorer overall survival in NPC patients.<sup>10,19</sup> Meanwhile, it has been documented that the levels of PD-L1 were upregulated in exosomes secreted by tumor cells in head and neck cancer, and that exosomal PD-L1 instead of soluble PD-L1 is responsible for the disease progression.<sup>14</sup>

The experimental observations manifested that PD-L1 expression was elevated by IFN- $\gamma$  secreted by inflammatory cells. In agreement with our finding, Chen et al. found that metastatic melanoma-derived exosomes, on IFN- $\gamma$  stimulation, expressed

more PD-L1, leading to suppressed antitumor responses.<sup>15</sup> Furthermore, our data demonstrated that PD-L1 binding to PD-1 was augmented by the IFN- $\gamma$  and inhibited by the anti-PD-L1 antibody. Regarding this, it has been established that upregulation of PD-L1 can enable tumor cells to mediate adaptive resistance to cytotoxic T lymphocyte-released IFN- $\gamma$ , which attributes to a vicious circle and exacerbates the malignancy.<sup>20</sup> PD-L1 binding to PD-1 is widely accepted to facilitate cancer immune escape via inhibition of T-cell functions, and, more recently, emerging data came to support that exosomal PD-L1 may induce tumor cell

**FIGURE 6** The graphical summary of the function and mechanism of PD-L1/PD-1 interaction in NPC immune escape. PD-L1 delivered by NPC patient plasma or NPC cell-derived exosomes can inhibit CD8+ T-cell activity by binding to PD-1 on the surface of CD8+ T cells, thus promoting NPC immune escape



immune escape and promote tumor progression in many cancers, such as breast cancer and glioblastoma.<sup>13,21</sup> In line with the aforementioned reports, mechanistic investigation of the current study delineated that PD-L1 bound to the PD-1 on CD8+ T-cell surface, accelerated the exhaustion of activated CD8+ T cells, and thereby exerted an immunosuppressive effect and contributed to the immune escape in NPC. Subsequent *in vivo* experiments further substantiated that exosomal PD-L1 promoted the growth of NPC cells in mice by attenuating CD8+ T-cell activity, which could be undermined by anti-PD-L1 antibody.

Although numerous previous studies have indicated that the exosomes from several types of cancer contain PD-L1 and show immune suppression both *in vitro* and *in vivo* to promote tumor development,<sup>13-15,21-24</sup> this study is the first to find that PD-L1 is highly expressed in the exosomes from the plasma of NPC patients and NPC cells, which can promote the immune escape of NPC cells by inhibiting the activity of CD8+ T cells, thereby promoting the occurrence and development of NPC. At the same time, although previous literature has shown that IFN- $\gamma$  in cancer cells can promote PD-L1 expression in the exosomes of cancer cells,<sup>15</sup> this study found that PD-L1 in exosomes inhibited IFN- $\gamma$  expression in CD8+ T cells.

Overall, this study is the first to demonstrate that PD-L1 carried by exosomes derived from NPC cells bound to the PD-1 on the CD8+ T-cell surface attenuate the activity of CD8+ T cells, thereby promoting the immune escape in NPC and ultimately contributing to the progression of NPC (Figure 6). This study deepens our understanding of molecular mechanisms underlying the immune escape of NPC cells and provides a new theoretical basis for the application of the anti-PD-1/PD-L1 immune checkpoint therapy for NPC, wherein binding of PD-1/PD-L1 can be blocked to reinvigorate the exhausted T cells, thus inhibiting NPC tumor growth. Further investigations are warranted in extracted primary NPC cells for experimental validation.

#### ACKNOWLEDGMENTS

This study was supported by the National Natural Science Foundation of China (Grant Nos 81902750 and 82002855) and the China Postdoctoral Science Foundation (Grant No. 2019M663293).

#### DISCLOSURE

The authors have no conflict of interest.

#### ORCID

Yahui Yu  <https://orcid.org/0000-0002-9104-8899>

#### REFERENCES

- Chia WK, Teo M, Wang WW, et al. Adoptive T-cell transfer and chemotherapy in the first-line treatment of metastatic and/or locally recurrent nasopharyngeal carcinoma. *Mol Ther*. 2014;22:132-139.
- Jia WH, Huang QH, Liao J, et al. Trends in incidence and mortality of nasopharyngeal carcinoma over a 20-25 year period (1978/1983-2002) in Sihui and Cangwu counties in southern China. *BMC Cancer*. 2006;6:178.
- Li YY, Chung GT, Lui VW, et al. Exome and genome sequencing of nasopharynx cancer identifies NF-kappaB pathway activating mutations. *Nat Commun*. 2017;8:14121.
- Perri F, Della Vittoria Scarpato G, Caponigro F, et al. Management of recurrent nasopharyngeal carcinoma: current perspectives. *Onco Targets Ther*. 2019;12:1583-1591.
- Ribas A, Wolchok JD. Cancer immunotherapy using checkpoint blockade. *Science*. 2018;359:1350-1355.
- Sharma P, Allison JP. The future of immune checkpoint therapy. *Science*. 2015;348:56-61.
- Banchereau R, Leng N, Zill O, et al. Molecular determinants of response to PD-L1 blockade across tumor types. *Nat Commun*. 2021;12:3969.
- Baumeister SH, Freeman GJ, Dranoff G, Sharpe AH. Coinhibitory pathways in immunotherapy for cancer. *Annu Rev Immunol*. 2016;34:539-573.
- Ribas A. Adaptive immune resistance: how cancer protects from immune attack. *Cancer Discov*. 2015;5:915-919.
- Jiang F, Yu W, Zeng F, et al. PD-1 high expression predicts lower local disease control in stage IV M0 nasopharyngeal carcinoma. *BMC Cancer*. 2019;19:503.
- Xie F, Xu M, Lu J, Mao L, Wang S. The role of exosomal PD-L1 in tumor progression and immunotherapy. *Mol Cancer*. 2019;18:146.
- Topalian SL, Taube JM, Anders RA, Pardoll DM. Mechanism-driven biomarkers to guide immune checkpoint blockade in cancer therapy. *Nat Rev Cancer*. 2016;16:275-287.
- Ricklefs FL, Alayo Q, Krenzlin H, et al. Immune evasion mediated by PD-L1 on glioblastoma-derived extracellular vesicles. *Sci Adv*. 2018;4:eaar2766.

14. Theodoraki MN, Yerneni SS, Hoffmann TK, Gooding WE, Whiteside TL. Clinical significance of PD-L1(+) exosomes in plasma of head and neck cancer patients. *Clin Cancer Res.* 2018;24:896-905.
15. Chen G, Huang AC, Zhang W, et al. Exosomal PD-L1 contributes to immunosuppression and is associated with anti-PD-1 response. *Nature.* 2018;560:382-386.
16. Wei Y, Zhao Q, Gao Z, et al. The local immune landscape determines tumor PD-L1 heterogeneity and sensitivity to therapy. *J Clin Invest.* 2019;129:3347-3360.
17. Zhang L, Yu D. Exosomes in cancer development, metastasis, and immunity. *Biochim Biophys Acta Rev Cancer.* 2019;1871:455-468.
18. Kalluri R. The biology and function of exosomes in cancer. *J Clin Invest.* 2016;126:1208-1215.
19. Zhou Y, Miao J, Wu H, et al. PD-1 and PD-L1 expression in 132 recurrent nasopharyngeal carcinoma: the correlation with anemia and outcomes. *Oncotarget.* 2017;8:51210-51223.
20. Garcia-Diaz A, Shin DS, Moreno BH, et al. Interferon receptor signaling pathways regulating PD-L1 and PD-L2 expression. *Cell Rep.* 2017;19:1189-1201.
21. Yang Y, Li CW, Chan LC, et al. Exosomal PD-L1 harbors active defense function to suppress T cell killing of breast cancer cells and promote tumor growth. *Cell Res.* 2018;28:862-864.
22. Del Re M, Marconcini R, Pasquini G, et al. PD-L1 mRNA expression in plasma-derived exosomes is associated with response to anti-PD-1 antibodies in melanoma and NSCLC. *Br J Cancer.* 2018;118:820-824.
23. Poggio M, Hu T, Pai CC, et al. Suppression of Exosomal PD-L1 induces systemic anti-tumor immunity and memory. *Cell.* 2019;177:414-427. e13.
24. Fan Y, Che X, Qu J, et al. Exosomal PD-L1 retains immunosuppressive activity and is associated with gastric cancer prognosis. *Ann Surg Oncol.* 2019;26:3745-3755.

#### SUPPORTING INFORMATION

Additional supporting information can be found online in the Supporting Information section at the end of this article.

**How to cite this article:** Yang J, Chen J, Liang H, Yu Y. Nasopharyngeal cancer cell-derived exosomal PD-L1 inhibits CD8+ T-cell activity and promotes immune escape. *Cancer Sci.* 2022;113:3044-3054. doi: [10.1111/cas.15433](https://doi.org/10.1111/cas.15433)